

From Defects to Photoluminescence in h-BN 2D and 0D Nanostructures

Plinio Innocenzi* and Luigi Stagi


 Cite This: *Acc. Mater. Res.* 2024, 5, 413–425

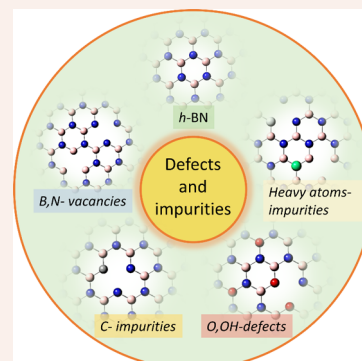

Read Online

ACCESS |

Metrics & More

Article Recommendations

CONSPECTUS: In the present Account, we report the recent progress of our research group on experimental and theoretical studies of defects in 2D and 0D hexagonal boron nitride. The studies of the effect of defects in boron-based structures have been also extended to boron oxide glasses. Engineering the different types of defects in h-BN is paramount because many functional properties of the material depend on them. This is particularly true for h-BN nanomaterials because of the main role played by surfaces. An important finding is that the formation of defects is directly dependent on the synthesis route; bottom-up or top-down syntheses generate different types of defects whose origins are generally connected to vacancies, dangling bonding, and substitutional oxygen impurities. We have focused our attention, in particular, on the correlation between defects and photoluminescence. The first part of this Account is dedicated to a general overview of defects that form in h-BN systems. In the second and third parts, we report on the rise of fluorescence in different types of h-BN nanostructures, in particular nanoflakes and BN dots. h-BN nanoflakes become fluorescent due to the presence of substitutional oxygen in the structure. The emission depends on the thermal processing of the material. A postsynthesis thermal treatment, because it induces the condensation of oxygen-related bonds that at the origin of fluorescence, changes the photoluminescence according to the degree of condensation of the structure. In the case of BN, the defects in dots and 0D nanostructures are discussed as a function of their preparation route. The analysis of defects in h-BN dots shows that not only vacancies and impurities can contribute to emission but also structural defects such as Stone–Wales. Understanding the origin of such defects and correlating them with specific optical properties is of the utmost importance because comprehending such phenomena could also guide the fabrication of new boron oxide emissive materials. In the last example, we show that the formation of defects, such as dangling bondings and vacancies, is the basis of a surprising phosphorescence at room temperature in boron oxide materials. We have observed, in particular, that the rise of boric acid phosphorescence after heat treatment is related to the presence of defects. The afterglow results from a trapping and detrapping process, which delays recombination at the active optical centers. The formation of near UV and blue optical transitions in absorption is revealed by a time-dependent density functional analysis of defective BOH molecules and clusters. In thermally processed boric acid samples, these defects cause photoluminescence.



1. INTRODUCTION

Hexagonal boron nitride (h-BN) is characterized by a honeycomb layered structure similar to that of graphene. The interplanar interactions in bulk h-BN (point group = D_{6h} ; space group = $P6_3/mmc$), as in graphite, are determined by van der Waals forces, while the B–N bonds maintain sp^2 hybridization and a weak ionic character compared with the purely covalent C–C bonding of graphite.¹ However, unlike the graphite pattern, the interlayer disposition of the BN sheets exhibits a displaced arrangement of atoms with boron atoms positioned above nitrogen. This structural arrangement affects the local polarity of the B–N bonds as well as the interlayer N-donor/B-acceptor characteristics.

The most common BN crystalline phases are h-BN, wurtzite w-BN, cubic c-BN, and rhombohedral r-BN, but the most stable, and therefore the most used in nanotechnologies, is the hexagonal one. The amorphous form of BN is noncrystalline

and lacks any long-range organization in analogy to amorphous carbon.

The h-BN form has a high thermal stability² to up to 1000 °C and only when treated in the 1000–1200 °C range transforms into B_2O_3 , even if the oxidation in h-BN nanosheets begins from 850 °C.³

h-BN is also classified as an indirect band gap semiconductor (E_g)⁴ with an energy gap close to 6 eV. This wide band gap enlarges the field of application to ultraviolet lasing,⁵

Received: November 13, 2023

Revised: March 1, 2024

Accepted: March 1, 2024

Published: March 15, 2024


Table 1. Synthesis Routes of h-BN, Generation Methods, and Optical Emission of Defects^a

synthesis route	types of defects	optical emission	notes
CVD	boron vacancies/substitutional boron	red SPEs (600–650 nm)	ammonia borane, borazine Cu/Fe/Pt/Ni catalysts ^{17–20}
MBE	N _B V _N antisite	a variety of emission lines (UV–vis range)	effusion source of B, N by a rf plasma source ⁵
LPE	oxygen/OH impurities	broad PL blue emission	bulk h-BN sonicated in water ³⁴
	Stone–Wales (SW) pentagon–heptagon defects	broad PL UV emission	bulk h-BN sonicated in H ₂ PO ₄ ²⁹
STE	boron/nitrogen vacancies; OH impurities	broad PL red/NIR emission (650–800 nm)	h-BN flakes irradiated by Xenon Plasma FIB in water ²⁰
	boron/nitrogen vacancies	red SPEs (608 nm)	nanoindentation on h-BN flakes and Ar annealing ²¹
	boron/nitrogen vacancies	green/yellow SPEs (535–588 nm)/blue SPEs (435 nm)	pulsed laser/electron beam irradiation of multilayered h-BN flakes ^{22–24}

^aCVD, chemical vapor deposition; MBE, molecular beam epitaxy; LPE, liquid-phase exfoliation; STE, scotch-tape exfoliation.

electronics,⁶ and photonics.⁷ Several types of nanostructures, from 2D to 0D, such as monolayers, nanoflakes, nanoribbons, nanotubes, dots, and nanocages up to fullerene-like molecules can be derived from h-BN.^{8,9} 2D materials can be deposited as monolayers, while nanoflakes and nanosheets are generally obtained via exfoliation of the bulk.¹⁰ Even if several protocols have been established, controlling the number of layers, dimensions, and defects remains a technological challenge. This is true not only for 2D structures but also for dots and 1D materials. The effective application of the fundamental properties of boron nitride in the nanoscale is made possible by fabricating high-quality h-BN nanomaterials with few or controlled defects, particularly for developing electrical and optoelectronic devices. Several advanced applications have envisaged for nanostructured h-BN as van der Waals heterostructures, heat dissipators in electronic devices, and single photon emitters in solid state quantum devices.

The formation of defects in h-BN is not limited to boron/nitrogen vacancies, but multiple defects can occur, such as carbon,¹¹ oxygen, and hydrogen impurities, boron/nitrogen vacancies,¹² and donor–acceptor pairs.¹³ The topological distribution of the defects is also significant, and edge defects, especially in 1D and 0D dimensions, become increasingly important. Defects can also be induced during h-BN processing because some specific functional properties, such as photoluminescence, depend on defects.

Numerous theoretical and experimental studies have examined the relationship between defects and photoluminescence. Defects cause fluorescence, whereas a defectless h-BN crystal exhibits no emission and a sharp band-to-band absorption edge. For example, single-photon emissions¹⁴ originate from atomic point defects and the identification of this characteristic contributed to the development of ultrabright, photostable, and broad-energy-range quantum emitters.^{15,16}

In this Account, we review our studies of defects in h-BN nanostructures, contextualizing them based on the current understanding of the relationships between structural defects and functional properties. In particular, the following aspects have been emphasized: defect formation, their control during material synthesis, and the correlation between defects and luminescence. These experimental results make it possible to achieve a better understanding of the complex physicochemical phenomena governing the properties of boron nitride on the nanoscale.

2. A GENERAL OVERVIEW OF DEFECTS IN H-BN NANOMATERIALS

Processing functional h-BN nanomaterials requires an in-depth understanding and mastery of defects, especially for applications in electronics and optoelectronics. Control of defects is crucial to reduce their presence when necessary and to modulate the material properties. The synthesis technique directly influences the type and the amount of defects, which can be of different nature. Indeed, defects can be related to the presence of anomalies in the regular lattice structure, and multiple defects such as carbon, oxygen, and hydrogen impurities and boron and nitrogen vacancies may also occur.

The defects are also not homogeneously distributed in the material, while the edges also play a primary role, because of dangling bonds.

Depending on the specific use case, the existence of imperfections, defined here broadly as structural elements causing h-BN to deviate from its ideal purity, may not necessarily exert a substantial influence or may even be advantageous. This underscores the importance of comprehending the methods to isolate particular defects and regulate their occurrence during the material's production process.

Inducing controlled structural defects in h-BN proves challenging. In general, fluorescent emissions from h-BN do not depend on electronic confinement effects due to nanometric size but rather on the presence of point defects and dislocations. Numerous defects typically arise randomly during h-BN synthesis, triggered by mechanical stress. These perturbations may promote the emergence of structural vacancies or the incorporation of new atoms, influenced by the choice of solvent during the exfoliation process or molecular precursors utilized in the synthesis. Obtaining h-BN nanomaterials involves two main approaches. Top-down synthesis, exemplified by “scotch-tape” (STE) and ball-milling methods, downsizes bulk material into nanoscale powder using external energy to break van der Waals forces. Solvent support enhances exfoliation and prevents sheet agglomeration. High-pressure microfluidization efficiently cleaves BN micropowders into thin fragments, yet challenges persist in achieving significant quantities for large-scale manufacturing. Chemical-assisted exfoliation, especially with sonication, is highly efficient, although the use of solvents, such as isopropyl alcohol (IPA) and N-methyl-2-pyrrolidone (NMP) may dope the structure with carbon impurities. While water is effective in BN exfoliation, it may lead to reactions and edge functionalization with OH. These approaches always provide structural defects whose percentage depends on the synthesis parameters. In particular, making use of organic solvents can promote carbon dimers and trimers that are supposed to emit in

UV and visible range.¹⁶ In the same way, OH and O defects can be introduced in the h-BN structure by using aqueous and acid solutions.^{29,50} The drawbacks of top-down approaches include the high difficulty of controlling the occurrence of unwanted defects and selectively introducing suitable impurities and vacancies. STE exfoliation presents a unique case, enabling the exfoliation of a few layers of a high-quality material. This process facilitates the introduction of specific luminescent structural defects through postprocessing, as illustrated in Table 1. In the bottom-up approach, material creation involves elemental or molecular components reacting and assembling. Chemical vapor deposition (CVD) ensures high-purity, low-defect layered materials by reacting BN molecular precursors such as borazine on substrates such as Pt (111) or Ni (111). Although CVD offers high-quality single BN sheets on various substrates, achieving large-scale usage and control over multiple layers remains challenging. Tailoring the BN film phases is achievable by selecting the appropriate substrate. Techniques such as pulsed layer deposition (PLD) or molecular beam epitaxy (MBE) may offer improvements in scalability. CVD and MBE techniques enable the control of adventitious impurities, establishing an initial structure onto which targeted defects can be incorporated through exposure to high-energy particles or laser light. Conversely, bottom-up approaches from solution, like those utilized in generating zero-dimensional h-BN, remain significantly reliant on molecular precursors and solvents that may introduce unwanted fluorescent impurities (Table 1).

2.1. Intrinsic Defects

Intrinsic h-BN defects have been the subject of numerous publications aimed at identifying fundamental aspects such as structural reorganization (deviation from flatness), electronic distribution, and optical absorption induced by intragap levels. Without considering foreign atoms, the B–N structure alone can give rise to various defects with unique properties. Most theoretical studies delve into the physical properties of potential color center candidates responsible for observed single-photon emissions in h-BN monolayers. We can encounter several theoretical approaches, such as group theory and density functional theory (DFT), which provide strong evidence that the electronic characteristics of these color centers match those observed experimentally. Group theory methods are used to compute the multielectron wave functions of the defects and conduct a detailed analysis of spin interactions. First-principle DFT methods can be employed to determine energy levels and zero-phonon-line (ZPL) emissions. The $V_N N_B$ neutral defect, consisting of a nitrogen vacancy near a nitrogen atom in boron sites, represents a peculiar defect within the hexagonal lattice in the framework of optical recombinations in the visible range. The suitability of the neutral $V_N N_B$ defect and negatively charged V_B defect as qubit candidates is based on their charge state's relative stability. In the energy range of $1.9 \text{ eV} < \epsilon_F < 2.6 \text{ eV}$, both the neutral $V_N N_B$ and neutral V_B defects exhibit equal stability. However, for $\epsilon_F > 2.6 \text{ eV}$, the negatively charged V_B defect becomes more stable. The $V_N N_B$ defect in h-BN is constrained to specific orientations at $\theta = 0^\circ, 120^\circ$, and 240° . Excitation of the $V_N N_B$ defect primarily occurs through the in-plane dipole moment, while the out-of-plane dipole moment can lead to excitations at energies around 2.0 eV. The excited $V_N N_B$ defect can return to the ground state through nonradiative and radiative shelving processes with the presence of a shelving state 4A1. The effective g-factor of the electronic spin remains consistent in both ground and excited states, leading to an

absence of Zeeman splitting in the photoluminescence spectrum of $V_N N_B$.²⁵ The latter has attracted great attention because of its potential application in quantum information. In particular, the importance of charged states of $V_N N_B$. Intentionally incorporating $V_N N_B$ defects into h-BN and achieving charged states of +1 and -1 could hold promise for quantum computing applications that tap into various defect states. In particular, $V_N N_B^{+1}$ and $V_N N_B^{-1}$ are anticipated to be capable of forming a durable quantum memory within h-BN, similar to the achievement seen with the defects in diamond.^{26,27}

First-principle density functional theory calculations have also been used to address the ultraviolet emission characteristics of pentagon–heptagon Stone–Wales defects^{28,29} and optically active square–octagon Stone–Wales line defects in h-BN.²⁸ These results imply a potential re-evaluation of fluorescent centers in h-BN, emphasizing the significance of the interplay between point defects and structural defects for comprehending the observed color centers in this material. Through DFT calculations, Hamdi et al.²⁸ observed that the pentagon–heptagon Stone–Wales defect in hexagonal boron nitride acts as an ultraviolet emitter, resembling a commonly observed 4.08 eV quantum emitter in polycrystalline h-BN. Similarly, the square–octagon Stone–Wales line defects in h-BN exhibit optical activity in the ultraviolet range. Ren et al.²⁹ investigated the synthesis process and the impact of the Brønsted acid treatment. Bulk h-BN powders were dispersed in orthophosphoric acid through sonication, followed by thermal treatment, leading to a highly defective crystal structure, evident in the emergence of UV emissions. Correspondingly, they focused on assessing the influence of Stone–Wales (SW) defects on both the structural and optical characteristics of an h-BN cluster system. The study utilized a simplified model comprising a hexagonal monolayer of h-BN with 61 rings and fully saturated edges, totaling 180 atoms. The introduction of defects involved inserting a pentagon–heptagon structure resulting from a B–N couple rotation, ensuring a constant total atom count in the cluster. Defect formation energies were computed in a neutral charge state. The defect-free cluster demonstrated robust optical absorption at 205 nm, in good agreement with the experimental data. The optimized structure displayed B–N bond lengths of 1.446 Å at the center and 1.419 Å at the edge. The incorporation of SW defects led to a redshift in optical absorption, with the most pronounced transition occurring at 283 nm when two or three SW defects were present. This redshift was attributed to deformations in the structure induced by the defects. The HOMO–LUMO transition in the defective BN(SW) system revealed a concentrated charge distribution around the SW defect. The formation energy of SW defects varied with the position in the cluster, with a preference for formation at the edge. In general, defects in h-BN nanostructures are studied in an indirect way by combining different spectroscopies or direct observation by high-resolution transmission electron microscopy. Combining X-ray photoelectron spectroscopy and near-edge X-ray absorption fine structure is also a powerful tool to investigate the formation of vacancies and has allowed researchers to identify the breaking of B–N bonds and the formation of N vacancies.³⁰

2.2. Carbon and Oxygen Defects

Much more relevant are the defects resulting from the treatment process of pure h-BN. As mentioned above, the solvent used for exfoliation can introduce atoms into the structure by promoting lower-energy optical absorption or facilitating photocatalytic

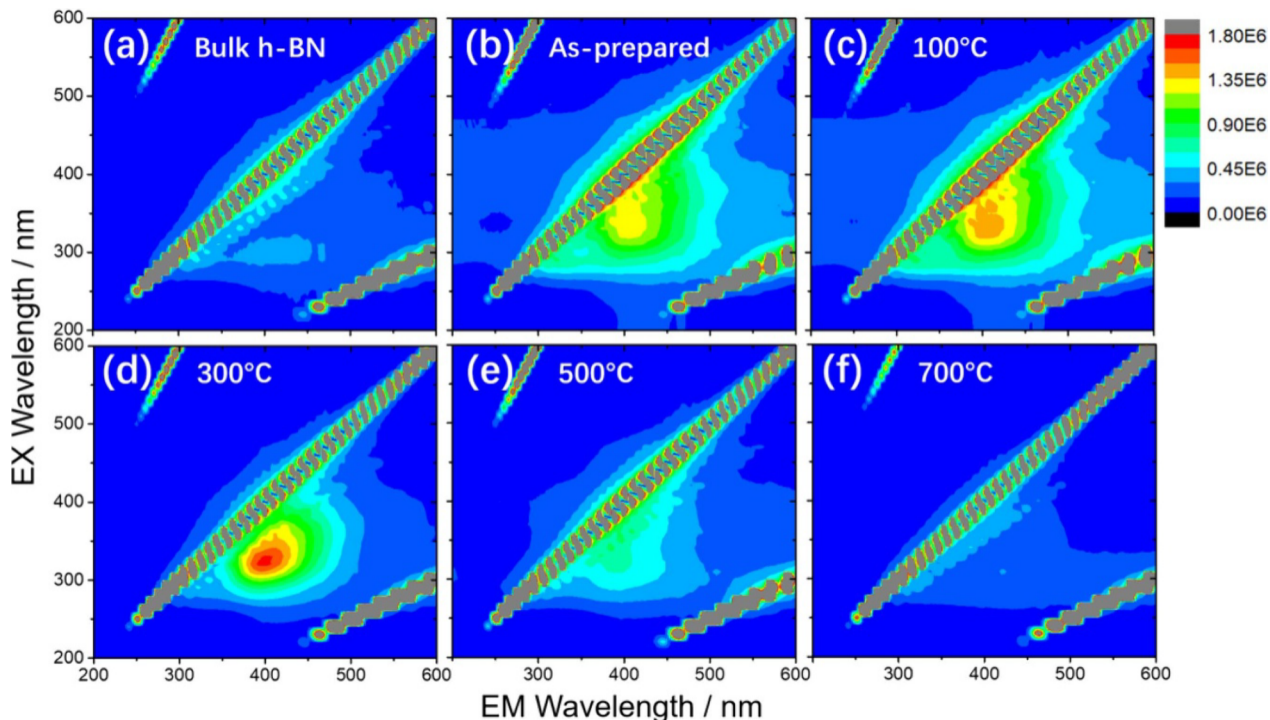


Figure 1. 3D PL excitation–emission intensity spectra of (a) bulk h-BN, (b) as-prepared h-BNNs, (c) 100 °C, (d) 300 °C, (e) 500 °C, and (f) 700 °C. In gray: first- and second-order artifacts. Reproduced with permission from ref 34. Copyright 2020 IOP Publishing, Ltd.

processes. Among the most common impurities that can be introduced are carbon and oxygen due to the use of organic solvents and water. The introduction of a substitutional carbon atom significantly changes the electronic properties compared to those of an undamaged boron nitride sheet. This substitution also leads to a notable decrease in the material work function. Defects create new electronic states within the energy gap, which strongly impact the h-BN optical properties. Additionally, the calculations show that the introduction of substitutional impurities or vacancy defects induces spin polarization in the structure. The calculations reveal a significant decrease in the work function compared with an undamaged h-BN sheet. The most significant reduction is observed with C_B and V_B defects, implying enhanced electron emission. Also, defects result in a narrower energy gap, and this reduction can be controlled by varying the defect concentration. The calculated spin density of states (DOS) shows that spontaneous magnetization occurs when substitutional impurities or vacancy defects are introduced into the structure.³¹ The defects $V_N C_B$ and $V_B C_N$ were also examined. $V_N C_B$ is suggested as a potential candidate for long-lived quantum memory, while $V_B C_N$ possesses a triplet ground state, rendering it suitable for tasks like spin initialization and quantum-qubit operations.²⁶ Winter et al. studied carbon dimers in h-BN. The luminescence zero-phonon energy of the carbon dimer defect is determined to be 4.36 eV, accounting for contributions from zero-point vibrational energy and reorganization energy. The presence of interlayer screening leads to a reduction in the emission energy by approximately 0.3 eV. The substitutional carbon dimer is identified as the probable source of the 4.1 eV luminescence line.³² Monomers, dimers, trimers, and CNO pairs are the most common carbon defects in h-BN. In contrast, larger carbon clusters and complexes involving vacancies and antisites are present in lower concentrations.³³ Clusters of BN free from defects exhibit optical transitions above 6 eV. The introduction of oxygen impurities induces a shift

toward longer wavelengths in band-to-band absorption. It leads to a reduction in the energy gap between the highest occupied molecular orbital (HOMO) and the lowest unoccupied molecular orbital (LUMO). Charged defects, such as oxygen impurities and $O_N V_B$ (oxygen–nitrogen–vacancy–boron) complexes, exhibit distinct mechanisms upon excitation. Interestingly, certain point defects exhibit varying mechanisms upon excitation, contingent on their type and charge. For instance, the positively charged ($q = +1$) oxygen impurities function as electron-withdrawing sites during HOMO-to-LUMO excitation, whereas the $2O_N$ and $O_N V_B$ complex act as recombination centers.³⁴

2.3. Heavy Metals

Foreign atom effects were also evaluated by investigating h-BN doped with heavy atoms.³⁵ Various wavelengths of interest for quantum technology applications were selected, including representations of solid-state quantum emitters and qubits in diamond and silicon carbide, quantum memories in rare-earth-ion-doped crystals, and alkali vapor-based memories. Additionally, wavelengths important for long-distance quantum communication in the telecom windows were considered. The study found suitable h-BN quantum emitters³⁶ for most of these applications, demonstrating promise for efficient coupling with other quantum systems. In some cases, charged defects were identified as potential candidates. However, defects such as SnBVB, ErBVB+, and ErB+, while technically not meeting the criteria for deep defects, could function as single photon emitters. It was noted that the AlN defect was the only one found at 637 nm, implying that it may emit the two-photon Fock state, potentially useful in quantum interference experiments. Similarly, the impact of isolated transition metal atoms (Sc, Ti, V, Cr, Mn, and Ni) embedded in h-BN as single-atom catalysts for CO oxidation was also considered. The findings suggest that Ni atoms show the most promising performance as

they have low barriers for both Langmuir–Hinshelwood (LH) and termolecular Eley–Rideal (TER) processes. This makes them suitable for operation at temperatures between 300 and 500 K.³⁷

3. DEFECT-ASSISTED PHOTOLUMINESCENCE IN H-BN LAYERS

As we previously pointed out, one of the most common top-down routes to obtain h-BN nanolayers is ultrasonic-assisted liquid-phase exfoliation (LPE). Ultrasonication, however, induces cavitation, i.e., the explosion and implosion of microbubbles, which promotes exfoliation through harsh and punctual changes in the pressure, temperature, and shear forces. A side effect of cavitation is inducing the formation of different types of defects, structural atomic vacancies, edge defects, and the B–OH species.³⁸ The solvent employed for the exfoliation is critical. Solvents such as dimethyl sulfoxide and *N*-methyl-2-pyrrolidone give almost defect-free h-BN sheets that are, in fact, not fluorescent, such as bulk h-BN. Water, instead, induces hydroxylation of nanostructured h-BN materials that, besides changing the optical properties, opens the possibility of further functionalization of the surface.³⁹

As-prepared h-BN sheets via PLE in water exhibit a weak photoluminescence in the blue (Figure 1).³⁴ The presence of defects characterizes the material due to the reaction with oxygen, as indicated by FTIR and Raman spectroscopy, particularly B–OH and N–B–O bonds. A direct assessment of the relationship between defects and luminescence is difficult to assess. In general, even if many theoretical calculations have been performed to understand the nature of defects and their effects on the optical properties, an experimental correlation is much more challenging to achieve. The data show the presence of two main defects; a possible strategy to understand their role is to try to reduce one of them and measure the eventual change in the optical response. This study can be done by thermal treatment in air that should reduce the content of B–OH groups by condensation. The result is an increase in the fluorescence up to 300 °C; higher temperatures, instead, produce a fluorescence quenching (Figure 1). The N–B–O defects contribute to the BN visible emission. These defects are unstable at higher temperatures and undergo a further oxidizing process that quenches the luminescence.

On the contrary, defect-free h-BN nanosheets prepared using DMSO and NMP as solvents do not exhibit oxygen defects and do not emit even after an oxidation treatment in air, demonstrating substantial thermal stability. Therefore, N–B–O oxygen defects are the key to controlling the photoluminescence (Figure 2). The rise of a specific infrared absorption band (460 cm^{-1}) with the increase of the thermal treatment temperature attributed to O–B–O bonds indicates

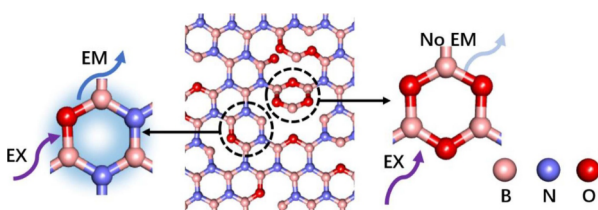


Figure 2. Schematic illustration for a possible fluorescent origin and mechanism from h-BN nanosheets. Reproduced with permission from ref 34. Copyright 2020 IOP Publishing, Ltd.

the transformation of N–B–O into the nonemissive boroxyl ring.

Theoretical calculations validated the experimental results. Computational methods have been used to derive the UV–vis absorption spectra of h-BN cluster models, introducing different defects in the structure, nitrogen and boron vacancies, and oxygen impurities (Table 2). The most probable candidates for interpreting the optical properties of defective h-BN nanosheets are charged oxygen defects because they create intragap transitions in absorption that accurately mimic the observed spectra.

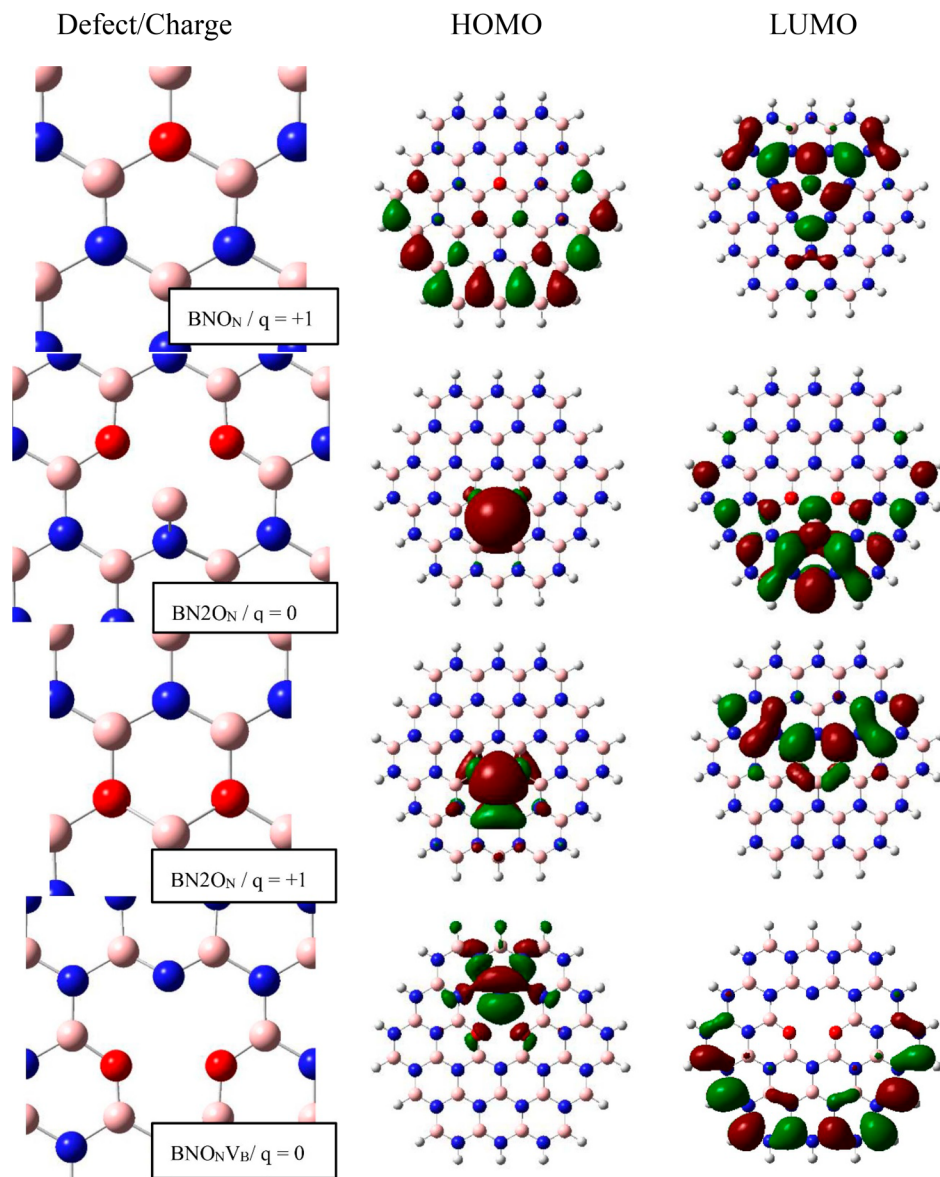
The formation of defects in exfoliated h-BN also affects other properties besides the photoluminescence. Several research groups have used 2D h-BN to enhance the photocatalytic response of photoactive materials such as titania.⁴⁰ Hexagonal boron nitride, however, is characterized by a large band gap and is not a suitable choice for such applications. The h-BN nanosheets are very soluble in water, and several solvents can be employed to process thin films via liquid phase deposition. This property allows integrating h-BN nanosheets into titania mesoporous films⁴¹ using a template-assisted sol–gel synthesis and evaporation-induced self-assembly⁴² (Figure 3). Interestingly, the 2D material can be incorporated into the films without disrupting the pore organization, while the layers remain optically transparent. The role of h-BN defects has been assessed by comparing the optical properties and the photocatalytic response of the heterostructures.⁴³ It has been discovered that the defects in h-BN improve the film photocatalytic activity because of the higher ultraviolet radiation A (UVA) absorption. Furthermore, the h-BN sheets support the crystallization of anatase by heterogeneous nucleation and are optically transparent but lack any photocatalytic property.

4. DEFECTS IN 0D H-BN NANOMATERIALS

BN dots exhibit a remarkable fluorescence that is usually attributed to different mechanisms correlated with radiative recombinations activated by the presence of defects, such as boron or nitrogen vacancies, carbene structures, and oxygen impurities.

The synthesis of 0D h-BN nanomaterials offers several choices regarding the available strategies. They can be top-down, starting with bulk h-BN, or bottom-up, with boron and nitrogen chemical precursors. Top-down routes, such as mechanical,⁴⁴ hydrothermal,⁴⁵ microwave,⁴⁶ sonication,⁴⁷ and exfoliation, are based on fragmenting h-BN sheets to obtain nano dots.⁴⁸ A typical bottom-up chemical method is the reaction of boric acid and ammonia under hydrothermal conditions. The bottom-up routes, however, do not allow, in general, to obtain pure BN dots, and the final material can contain several foreign atoms such as oxygen (boron oxynitride) or carbon or a combination of both (carbon boron oxynitride) and hydrogen. Carbon, oxygen, and hydrogen impurities enter the BN structure throughout the preparation process, and their presence can be somewhat controlled.

Defects in BN dots are also fundamental to modulating the optical properties.⁴⁹ In the case of hydrothermal synthesis from H_3BO_3 and NH_3 , used as precursors of boron and nitrogen, respectively, the final material is more correctly identified as a boron oxynitride dot (BOND).⁵⁰ Interestingly, such dots can show a two-color emission (Figure 4). The emission of the two components decreases in intensity with the increase in thermal treatment temperature. The condensation of the structure decreases the number of defects and in turn quenches the

Table 2. Representation of HOMO and LUMO^a

^aReproduced with permission from ref 29. Copyright 2021 Elsevier.

fluorescence. The emission remains stable at 25 °C, and the BONs can be incorporated into a solid-state matrix to fabricate thin emitting films via sol–gel processing. The synthesis of BN dots from a top-down route opens a different scenario. Controlling the amount of impurities proves difficult in bottom-up syntheses, and in general, the functions of the final product are regulated by the amount and types of impurities, as well as the defects commonly found in boron nitride structures. In top-down syntheses of BN dots, the process is similar to that used to obtain 2D materials. Bulk h-BN powders are exfoliated and fragmented by cavitation via sonication, but ball-milling, solvothermal, or microwave treatments are also suitable routes. The solvents employed represent a key point of the process. Water, ethylene glycol, dimethylformamide (DMF), and 1-methyl-2-pyrrolidone (NMP) are among the most common, but organic solvents have the drawback that carbon, oxygen, and hydrogen impurities can enter into the B–N structure of the dots. The presence of carbon atoms is a source of uncertainty in modulating and understanding the optical and structural

properties of the h-BN systems. To avoid an uncontrolled presence of carbon, the BN bulk material must be exfoliated with a carbon-free liquid phase but also in this case formation of defects should be expected. We created luminescent BN dots via a two-step protocol by heating bulk h-BN in H₃PO₄ and then treating the resultant product in an ultrasonic bath for several hours. The synthesized BN dots share structural features with bulk h-BN but exhibit novel optical and vibrational properties that are tightly correlated.

To form h-BN nanodots, h-BN powders are at first dispersed in a solution of concentrated H₃PO₄ and then thermally treated at 200 °C for 1 h. Then, the dispersion was ultrasonicated for 15 h and the larger h-BN particles removed by centrifugation. In the final step, BN dots were purified by dialysis and filtered. This procedure has allowed obtaining BN dots with very peculiar optical properties. The fluorescence spectra (Figure 5), in fact, show a quite surprising emission in the UV in the as-prepared samples. The emission changes according to the thermal treatment in oxidizing conditions from 25 up to 300 °C. No

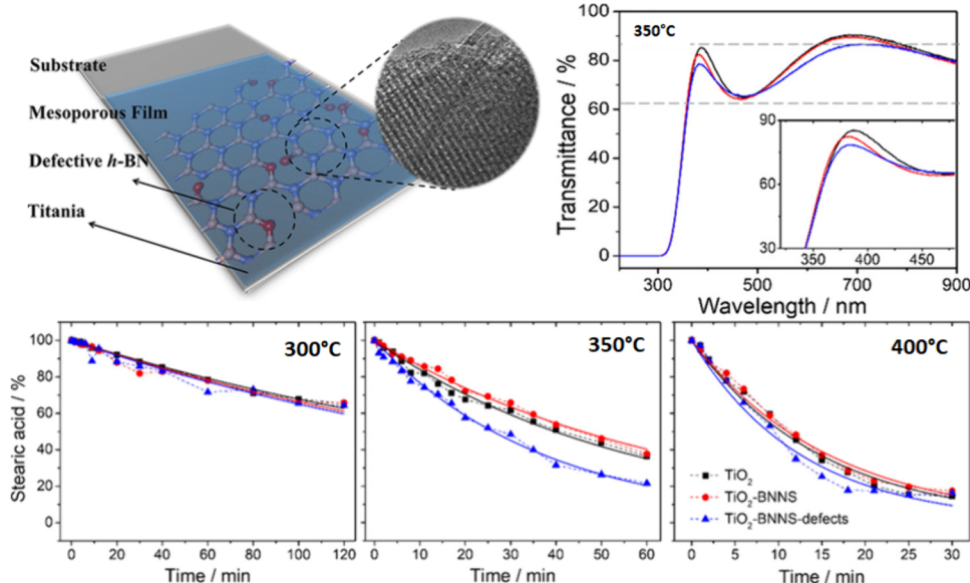


Figure 3. (top right) UV–vis transmission spectra of mesoporous films: TiO_2 (black line), $\text{TiO}_2\text{-BN}$ (red line), and $\text{TiO}_2\text{-BN}$ with defects (blue line) after thermal treatment at 350 °C. (bottom) Photodegradation of stearic acid onto TiO_2 mesoporous films (black line), $\text{TiO}_2\text{-BN}$ (red line), and $\text{TiO}_2\text{-BN}$ (blue line) films treated at 300, 350, and 400 °C. Reproduced with permission from ref 42. Copyright 2020 American Chemical Society.

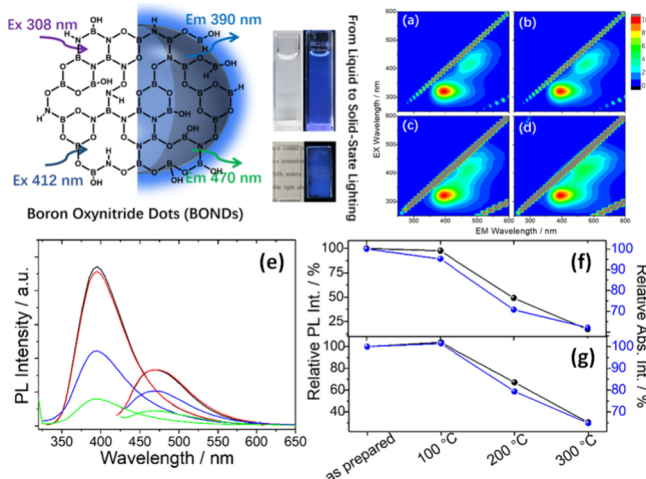


Figure 4. (top left) Schematic of the boron oxynitride dots (BONDS). (top right) 3D PL excitation–emission intensity spectra of (a) BONDS, (b) 100 °C, (c) 200 °C, and (d) 300 °C (in water, 0.1 mg mL⁻¹). (bottom left) (e) Emission spectra of the two components upon excitation at $\lambda_{\text{ex}} = 308$ and 412 nm. (bottom right) (f) The relative emission and absorption intensities of the band peaking at 390 (black line) and 308 nm (blue line), respectively. (g) The relative emission and absorption intensities of the band peaking at 470 (black line) and 412 nm (blue line), respectively. Reproduced with permission from ref 50. Copyright 2020 Elsevier.

UV emission will be detected if the h-BN particles are heated or sonicated. Instead, the UV emission is detectable only after heating and sonication in acid.

In pristine BN dots, two distinct emissions are observed: the first one is in the UV range from 300 to 370 nm with excitation at 270 nm, while the second band goes from 370 to 530 nm with excitation and emission maxima at 310 and 420 nm, respectively. Blue emission may also be stimulated by 270 nm irradiation, resulting in a distinctive UV–blue double fluorescence. The blue emission reaches a maximum at 200 °C, in perfect accordance with what is observed in the BN dots obtained via bottom-up

synthesis. The origin of such an emission is therefore attributed to structural defects connected with B–OH species. The UV emission, instead, is more intriguing, and its correlation with a specific defect is not straightforward. The UV photoluminescence, at 260 nm, depends on peculiar structural defects that form in the BN crystal lattice, irrespective of the particular morphology. The infrared absorption spectra demonstrate a specific correlation between fluorescence and structural properties (Figure 6).

The characteristic in-plane B–N stretching at 1372 cm⁻¹ (Figure 6) appears formed by two overlapping components, an almost temperature-independent mode at 1372 cm⁻¹ and a second band at 1383 cm⁻¹, which monotonically decrease in intensity with the temperature and disappear at 250 °C. The difference between the infrared spectra of as-made BN and the dots prepared at 250 °C indicates the presence of a sharp band (Figure 6d). This infrared band is correlated to the UV emission at 320 nm; in fact, the thermal treatment promotes a decrease in both UV fluorescence and the 1383 cm⁻¹ band. This suggests that a direct correspondence exists between the physical properties of the two dots. The splitting of the in-plane B–N stretching infrared band should be correlated to changes of the intrinsic hexagonal crystal structure; therefore, a characteristic defect and the consequent local deformation of the lattice that affects the BN in-plane vibrational features should exist. This defect causes UV fluorescence emission connected with saturating –OH and –H groups. Stone–Wales defects, created by rotating a B–N pair by 90°, might be the source of the UV emission. DFT studies have demonstrated that pentagon–heptagon Stone–Wales (SW) defects with optical transitions at roughly 4 eV can form due to the favorable energy conditions of substantial strain at the grain boundaries (Figure 7).

The synthesis and outcome of the Brønsted acid treatment are summarized in Section 5. Via sonication for a few minutes, the h-BN bulk powders dissolve throughout a concentrated orthophosphoric acid solution. The intercalation and interaction of H_3PO_4 with the BN structure are facilitated by the heat treatment at 200 °C, which is near the boiling point of around

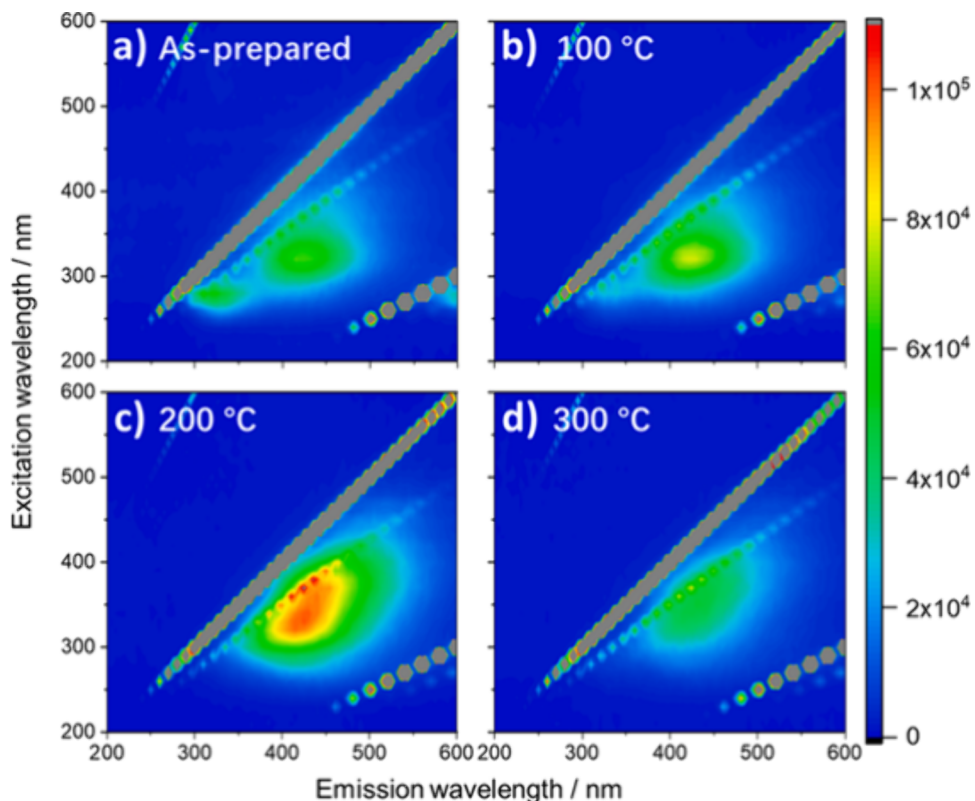


Figure 5. (a–d) 3D PL excitation (y-axis)–emission (x-axis) intensity spectra in the 200–600 nm ranges of as-prepared BN dots and thermally treated dots at different temperatures. The intensity is shown as a false color scale. The gray lines are artifacts generated by first- and second-order excitation. Reproduced with permission from ref 50. Copyright 2020 Elsevier.

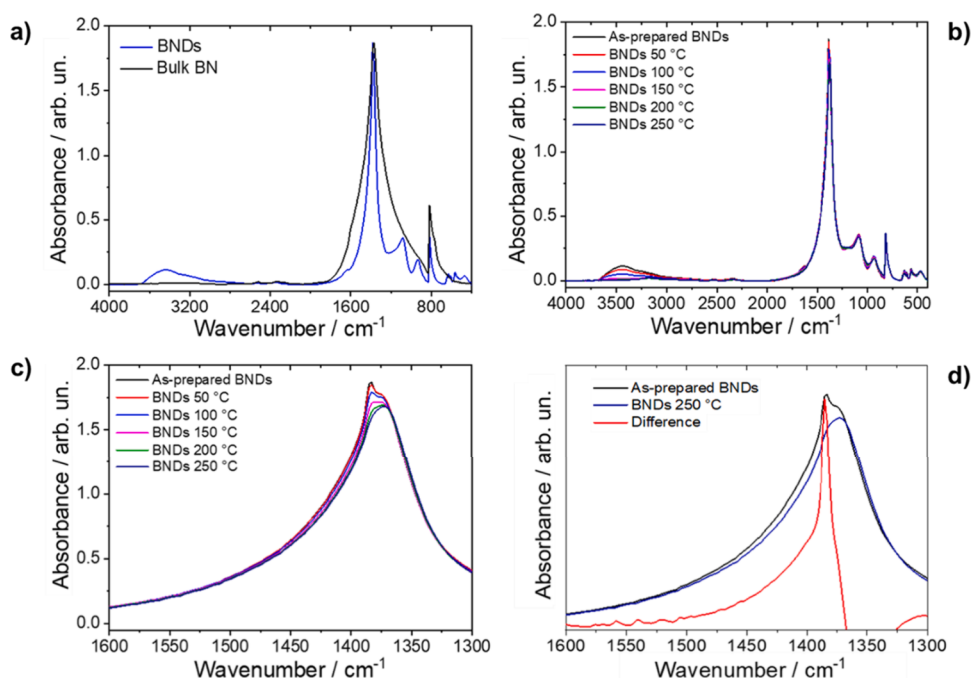


Figure 6. (a) FTIR absorption spectra of bulk h-BN powder (black curve) and BNDs (blue curve). (b) In situ FTIR spectra as a function of temperature. (c) Enlarged spectra in the 1600–1300 cm⁻¹ range. The spectra show an additional overlapped sharp band peak at 1383 cm⁻¹. (d) Spectral difference between the as-prepared BNDs and the dots treated at 250 °C. The sharp absorption band (red line) results from the difference. Reproduced with permission from ref 50. Copyright 2020 Elsevier.

212 °C. B–N bonds break as a result of the intense oxidation that follows, particularly at the edges and exposed surfaces. The unsaturated bonds can work as anchor sites for –OH groups and

protons. At the end of the process, the crystal structure appears highly defective as demonstrated by the emergence of UV emissions. The stressed and defective crystalline lattice can be

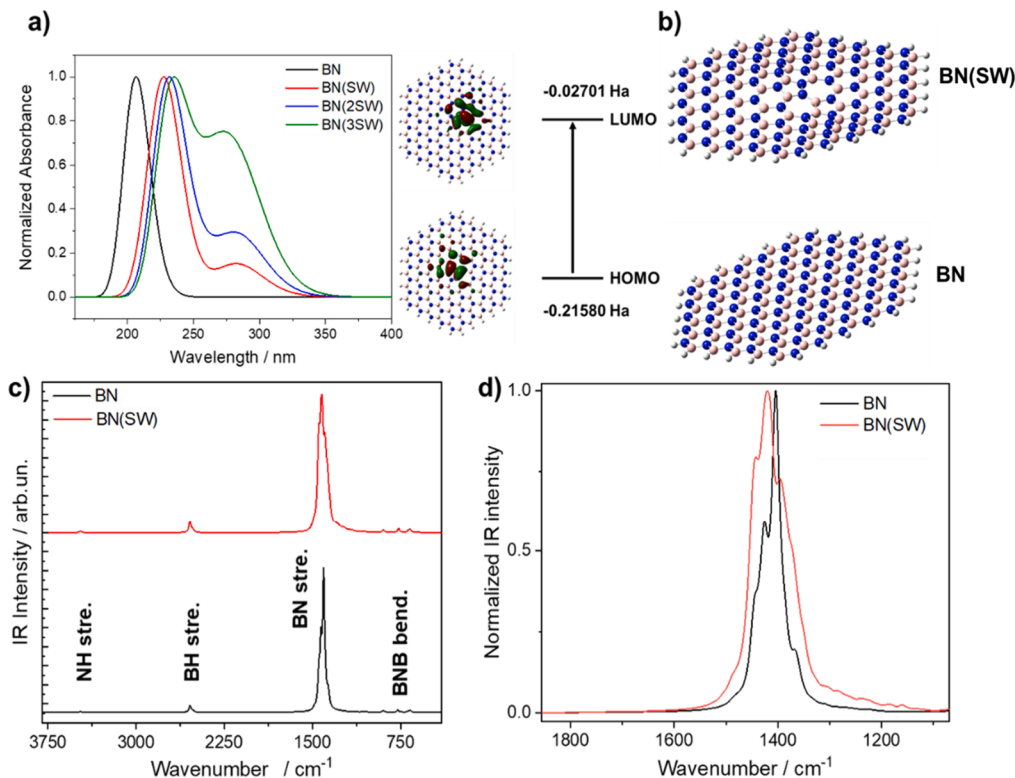


Figure 7. (a) Computed UV–vis absorption of pristine (BN) and defective h-BN (BN(SW)) clusters in the presence of two and three Stone–Wales (SW) defects and HOMO–LUMO representations of the computed defects. (b) Representation of optimized BN and BN(SW) structures with the defect-related structural deformation that bends the planar geometry of the BN cluster. (c and d) Calculated infrared spectra of BN (black line) and BN(SW) (red line) clusters. Reproduced with permission from ref 50. Copyright 2020 Elsevier.

further oxidized and strain-relaxed by high-temperature annealing.

5. FROM BN DEFECTS TO BORON OXIDE, STRUCTURAL DEFECTS AT ORIGIN OF PHOSPHORESCENCE

The correlation between defects and photoluminescence properties in BN structures suggests that defects can also play a major role in pure boron oxide materials. A puzzling phenomenon is the room temperature phosphorescence observed in B_2O_3 . Several research groups have observed the rise of such fluorescence, which is explained by the possible presence of defects. Based on experiments performed on boron nitride nanostructures, it was hypothesized that this effect may also be directly related to the formation of structural defects in boron oxide.⁵¹ The investigation of boron oxide phase transitions during heat treatments at increasing temperatures revealed the occurrence of structural modifications when H_3BO_3 melts and afterward recrystallizes (Figure 8).

The blue and green optical centers are compatible with forming structural defects of oxygen vacancies and unsaturated bonds. They are formed during the melting and recrystallization process and reduce their occurrence by treatment at higher temperatures, where the oxide phase is predominant.

Boron oxide samples treated between 200 and 400 °C display exceptional phosphorescence in the visible spectrum. Two different phosphorescent emissions occur at around 480 and 528 nm, related to trapped charge carrier recombinations detected by thermoluminescence and electron paramagnetic resonance spectroscopy (EPR) (Figure 9). The afterglow is caused by a trapping and detrapping mechanism that slows down the

recombination at active optical centers. A time-dependent density functional analysis of defective BOH molecules and clusters reveals the formation of near UV and blue optical transitions. The experimental findings well support the hypothesis that the thermal processing of boric acid induces defects that become centers of luminescence and recombination channels in the visible spectrum. This explains why boric acid samples treated between 200 and 400 °C show significant phosphorescence in the visible range. Two distinctive phosphorescent emissions are observed at around 480 and 528 nm. These emissions are linked to the recombination of trapped charge carriers as determined by electron paramagnetic resonance spectroscopy and thermoluminescence. Trapping and detrapping occur, delaying the recombination at the active optical centers and producing the afterglow. Time-dependent density functional analysis of defective BOH molecules and clusters reveals near UV and blue absorptions. In thermally treated boric acid samples, these defects cause photoluminescence.

6. CONCLUSIONS AND PERSPECTIVES

The formation and control of defects in h-BN nanostructures are the basis of great interest in this material. Defects can be obtained as an uncontrolled side effect of the manufacturing process or intentionally introduced. In two-dimensional nanostructures obtained via bottom-up processes, defect control is also much more difficult because exfoliation processes do not allow for precise control of nanostructures in terms of size, layer thickness, and shape. The defects that generate photoluminescence are closely related, as we have described, to the presence of different types of defects that are observed in both

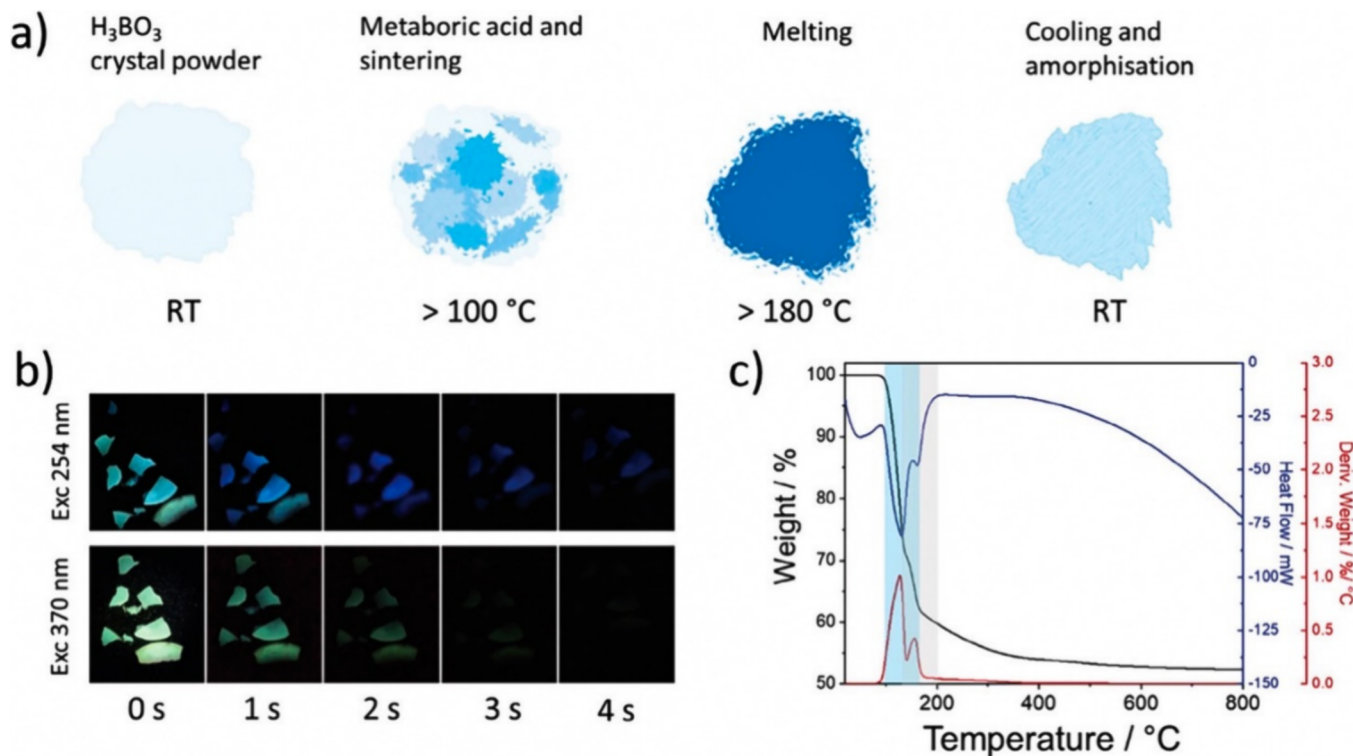


Figure 8. (a) Sketch of boric acid thermal treatment that gives phosphorescence. At room temperature, boric acid does not emit, but after recrystallization at temperatures higher than 180 °C, it becomes phosphorescent. (b) Images of phosphorescent samples after thermal treatment at 250 °C acquired with a camera at 1 s intervals after two different excitation wavelengths, 254 and 370 nm; 0 s corresponds to the instant of switching off the source. (c) DSC-TGA analysis of as-purchased H₃BO₃. Gray and light blue areas highlight the temperature interval between the two H₃BO₃ dehydration processes. Reproduced from ref 51. Copyright 2023 Wiley.

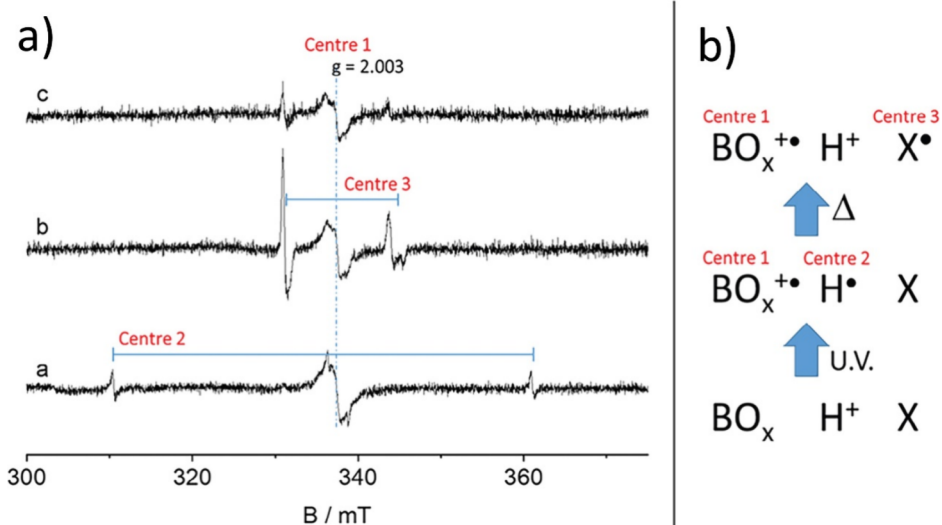


Figure 9. (a) EPR spectra of sample treated at 250 °C, (a) under UV irradiation, (b) after exposing the EPR cell to room temperature, and (c) after 1 day at room temperature. (b) Sketch of the processes related to the spectra evolution in panel (a) and involving a boron-containing structural defect (BO_x), an isolated proton, and a further not assigned defect X. Reproduced from ref 51. Copyright 2023 Wiley.

nanosheets and h-BN dots. Understanding the direct defect–property correspondence on the nanoscale is critical in the use of such materials. Combining experimental methods and theoretical calculations is the best solution to this problem. In this Account, we have seen how the presence of defects in nanostructures is strongly influenced by heat treatment. While this property, on one hand, makes it possible to detect defects accurately, it also shows limitations in using such materials due

to limited thermal stability. The defects indeed depend on the process used to obtain boron nitride nanomaterials. An important point to stress is that defects can be not only vacancies or impurities but also structural defects in honeycomb structures, such as that of h-BN, which can make a significant contribution to changing the material functional properties.

Much of the research in this area is focused on controlling defects in monolayers, but as we have seen, the emission of

nanosheets and dots is also created by defects. Dangling bonding and vacancies in the presence of oxygen generate these defects. The next step will be to generate these defects in a controlled manner, even considering that the possible applications of such materials as emissive nanostructures do not require spatial control of the defects. The importance of such an approach has been also illustrated by the last example reported in the Account that regards boron oxide. Formation of optically active defects can generate phosphorescence at room temperature, which has been previously attributed to impurities. More investigations are necessary to fully exploit the potential of optically active h-BN nanostructures, but defects are certainly the key.

■ AUTHOR INFORMATION

Corresponding Author

Plinio Innocenzi – *Laboratory of Materials Science and Nanotechnology (LMNT), Department of Biomedical Sciences, CR-INSTM, University of Sassari, 07100 Sassari, Italy; [ORCID iD](https://orcid.org/0000-0003-2300-4680); Email: plinio@uniss.it*

Author

Luigi Stagi – *Laboratory of Materials Science and Nanotechnology (LMNT), Department of Biomedical Sciences, CR-INSTM, University of Sassari, 07100 Sassari, Italy; [ORCID iD](https://orcid.org/0000-0002-7238-8425)*

Complete contact information is available at:
<https://pubs.acs.org/10.1021/accountsmr.3c00242>

Notes

The authors declare no competing financial interest.

Biographies



Plinio Innocenzi is full professor of materials science at the University of Sassari and Director of the Laboratory of Materials Science and Nanotechnology. He studied physics at the University of Padova and did his postdoc at the University of Kyoto in Japan from 1993 to 1996. He has published more than 240 scientific articles on nanoscience and sol-gel and hybrid organic-inorganic chemistry. His research interests include nanomaterials for photonics and biotechnologies synthesised via chemical routes.



Luigi Stagi is a research fellow at the University of Sassari. He is an assistant professor (RTDA) in the Department of Biomedical Science, University of Sassari (Italy). In 2021, he was a visiting scientist at Georg-August-Universität Göttingen (Germany). He earned a Ph.D. in physics at the University of Cagliari (Italy). His research is focused on the structural and optical properties of low-dimensional materials, and the results have been reported in more than 50 publications in peer-reviewed international journals.

■ ACKNOWLEDGMENTS

This work was funded and it has been developed within the framework of the project e.INS-Ecosystem of Innovation for Next Generation Sardinia (Grant ECS 00000038) funded by the Italian Ministry for Research and Education (MUR) under the National Recovery and Resilience Plan (NRRP) MISSION 4 COMPONENT 2, “From Research to Business” IN-VESTMENT 1.5, “Creation and Strengthening of Ecosystems of Innovation”, and construction of “Territorial R&D Leaders”. The authors also acknowledge funding from MUR under the PRIN Project 2022LZWKAJ.

■ REFERENCES

- (1) Yu, C.; Zhang, J.; Tian, W.; Fan, X.; Yao, Y. Polymer composites based on hexagonal boron nitride and their application in thermally conductive composites. *RSC Adv.* **2018**, *8*, 21948.
- (2) Sharma, V.; Kagdada, H. L.; Jha, P. K.; Śpiewak, P.; Kurzydłowski, K. J. Thermal transport properties of boron nitride based materials: A review. *Ren. Sust. Energy Rev.* **2020**, *120*, 109622.
- (3) Li, L. H.; Cervenka, J.; Watanabe, K.; Taniguchi, T.; Chen, Y. Strong Oxidation Resistance of Atomically Thin Boron Nitride Nanosheets. *ACS Nano* **2014**, *8*, 1457–1462.
- (4) Cassabois, G.; Valvin, P.; Gil, B. Hexagonal boron nitride is an indirect bandgap semiconductor. *Nat. Photonics* **2016**, *10*, 262–266.
- (5) Watanabe, K.; Taniguchi, T.; Kanda, H. Direct-bandgap properties and evidence for ultraviolet lasing of hexagonal boron nitride single crystal. *Nat. Mater.* **2004**, *3*, 404–409.
- (6) Moon, S.; Kim, J.; Park, J.; Im, S.; Kim, J.; Hwang, I.; Kim, J. K. Hexagonal Boron Nitride for Next-Generation Photonics and Electronics. *Adv. Mater.* **2023**, *35*, 2204161.
- (7) Caldwell, J. D.; Aharonovich, I.; Cassabois, G.; Edgar, J. H.; Gil, B.; Basov, D. N. Photonics with hexagonal boron nitride. *Nat. Rev. Mater.* **2019**, *4*, 552–567.
- (8) Gonzalez-Ortiz, D.; Salameh, C.; Bechelany, M.; Miele, P. Nanostructured boron nitride-based materials: synthesis and applications. *Mater. Today Adv.* **2020**, *8*, 100107.
- (9) Arenal, R.; Lopez-Bezanilla, A. Boron nitride materials: an overview from 0D to 3D (nano)structures. *Wires Comput. Mol. Sci.* **2015**, *5*, 299–309.
- (10) Gautam, C.; Chelliah, S. Methods of hexagonal boron nitride exfoliation and its functionalization: covalent and non-covalent approaches. *RSC Adv.* **2021**, *11*, 31284–31327.

- (11) Tawfik, S. A.; Ali, S.; Fronzi, M.; Kianinia, M.; Tran, T. T.; Stampfl, C.; Aharonovich, I.; Toth, M.; Ford, M. J. First-principles investigation of quantum emission from hBN defects. *Nanoscale* **2017**, *9*, 13575–13582.
- (12) Reimers, J. R.; Shen, J.; Kianinia, M.; Bradac, C.; Aharonovich, I.; Ford, M. J.; Piecuch, P. Photoluminescence, photophysics, and photochemistry of the V B- defect in hexagonal boron nitride. *Phys. Rev. B* **2020**, *102*, 144105.
- (13) Mackoit-Sinkevičienė, M.; Maciaszek, M.; van de Walle, C. G.; Alkauskas, A. Carbon dimer defect as a source of the 4.1 eV luminescence in hexagonal boron nitride. *Appl. Phys. Lett.* **2019**, *115*, 212101.
- (14) Bourrellier, R.; Meuret, S.; Tararan, A.; Stéphan, O.; Kociak, M.; Tizei, L. H. G.; Zobelli, A. Bright UV Single Photon Emission at Point Defects in h-BN. *Nano Lett.* **2016**, *16* (7), 4317–4321.
- (15) Reserbat Plantey, A.; Epstein, I.; Torre, I.; Costa, A. T.; Gonçalves, P. A. D.; Mortensen, N. A.; Polini, M.; Song, J. C. W.; Peres, N. M. R.; Koppens, F. H. L. Quantum Nanophotonics in Two-Dimensional Materials. *ACS Photonics* **2021**, *8*, 85–101.
- (16) Aharonovich, I.; Tetienne, J.-P.; Toth, M. Quantum Emitters in Hexagonal Boron Nitride. *Nano Lett.* **2022**, *22*, 9227–9235.
- (17) Abidi, I. H.; Mendelson, N.; Tran, T. T.; Tyagi, A.; Zhuang, M.; Weng, L.-T.; Özylmaz, B.; Aharonovich, I.; Toth, M.; Luo, Z. Selective Defect Formation in Hexagonal Boron Nitride. *Adv. Optical Mater.* **2019**, *7*, 1900397.
- (18) Mendelson, N.; Xu, Z.-Q.; Tran, T. T.; Kianinia, M.; Scott, J.; Bradac, C.; Aharonovich, I.; Toth, M. Engineering and Tuning of Quantum Emitters in Few-Layer Hexagonal Boron Nitride. *ACS Nano* **2019**, *13*, 3132–3140.
- (19) Stern, H. L.; Wang, R.; Fan, Y.; Mizuta, R.; Stewart, J. C.; Needham, L.-M.; Roberts, T. D.; Wai, R.; Ginsberg, N. S.; Klenerman, D.; Hofmann, S.; Lee, S. F. *ACS Nano* **2019**, *13*, 4538–4547.
- (20) Glushkov, E.; Macha, M.; Räth, E.; Navikas, V.; Ronceray, N.; Cheon, C. Y.; Ahmed, A.; Avsar, A.; Watanabe, K.; Taniguchi, T.; Shorubalko, I.; Kis, A.; Fantner, G.; Radenovic, A. Engineering Optically Active Defects in Hexagonal Boron Nitride Using Focused Ion Beam and Water. *ACS Nano* **2022**, *16*, 3695–3703.
- (21) Xu, X.; Martin, Z. O.; Sychev, D.; Lagutchev, A. S.; Chen, Y. P.; Taniguchi, T.; Watanabe, K.; Shalaev, V. M.; Boltasseva, A. Creating Quantum Emitters in Hexagonal Boron Nitride Deterministically on Chip-Compatible Substrates. *Nano Lett.* **2021**, *21*, 8182–8189.
- (22) Gan, L.; Zhang, D.; Zhang, R.; Zhang, Q.; Sun, H.; Li, Y.; Ning, C.-Z. Large-Scale, High-Yield Laser Fabrication of Bright and Pure Single-Photon Emitters at Room Temperature in Hexagonal Boron Nitride. *ACS Nano* **2022**, *16*, 14254–14261.
- (23) Kumar, A.; Cholsuk, C.; Zand, A.; Mishuk, M. N.; Matthes, T.; Eilenberger, F.; Suwanna, S.; Vogl, T. Localized creation of yellow single photon emitting carbon complexes in hexagonal boron nitride. *APL Mater.* **2023**, *11*, 071108.
- (24) Fournier, C.; Plaud, A.; Roux, S.; Pierret, A.; Rosticher, M.; Watanabe, K.; Taniguchi, T.; Buil, S.; Quélin, X.; Barjon, J.; Hermier, J.-P.; Delteil, A. Position-controlled quantum emitters with reproducible emission wavelength in hexagonal boron nitride. *Nat. Commun.* **2021**, *12*, 3779.
- (25) Abdi, M.; Chou, J. P.; Gali, A.; Plenio, M. B. Color Centers in Hexagonal Boron Nitride Monolayers: A Group Theory and Ab Initio Analysis. *ACS Photonics* **2018**, *5*, 1967–1976.
- (26) Sajid, A.; Reimers, J. R.; Kobayashi, R.; Ford, M. J. Theoretical Spectroscopy of the VNNB Defect in Hexagonal Boron Nitride. *Phys. Rev. B* **2020**, *102* (14), n/a.
- (27) Li, S.; Chou, J.-P.; Hu, A.; Plenio, M. B.; Udvaryhelyi, P.; Thiering, G.; Abdi, M.; Gali, A. Giant shift upon strain on the fluorescence spectrum of VNNB color centers in h-BN. *npj Quantum Inf.* **2020**, *6*, 85.
- (28) Hamdi, H.; Thiering, G.; Bodrog, Z.; Ivády, V.; Gali, A. Stone-Wales Defects in Hexagonal Boron Nitride as Ultraviolet Emitters. *npj Comput. Mater.* **2020**, *6*, 1–7.
- (29) Ren, J.; Stagi, L.; Malfatti, L.; Carbonaro, C. M.; Granozzi, G.; Calvillo, L.; Garroni, S.; Enzo, S.; Innocenzi, P. Engineering UV-Emitting Defects in h-BN Nanodots by a Top-down Route. *Appl. Surf. Sci.* **2021**, *S67*, 150727.
- (30) Petracic, M.; Peter, R.; Fan, L.-J.; Yang, Y.-W.; Chen, Y. Direct observation of defects in hexagonal boron nitride by near-edge X-ray absorption fine structure and X-ray photoemission spectroscopy. *Nucl. Instrum. Methods Phys. Res.* **2010**, *619*, 94–97.
- (31) Azevedo, S.; Kaschny, J. R.; De Castilho, C. M. C.; De Brito Mota, F. Electronic Structure of Defects in a Boron Nitride Monolayer. *Eur. Phys. J. B* **2009**, *67* (4), 507–512.
- (32) Winter, M.; Bousquet, M. H. E.; Jacquemin, D.; Duchemin, I.; Blase, X. Photoluminescent Properties of the Carbon-Dimer Defect in Hexagonal Boron-Nitride: A Many-Body Finite-Size Cluster Approach. *Phys. Rev. Mater.* **2021**, *5* (9), n/a.
- (33) Maciaszek, M.; Razinkovas, L.; Alkauskas, A. Thermodynamics of Carbon Point Defects in Hexagonal Boron Nitride. *Phys. Rev. Mater.* **2022**, *6* (1), 1–13.
- (34) Ren, J.; Stagi, L.; Carbonaro, C. M.; Malfatti, L.; Casula, M. F.; Ricci, P. C.; Del Rio Castillo, A. E.; Bonaccorso, F.; Calvillo, L.; Granozzi, G.; Innocenzi, P. Defect-Assisted Photoluminescence in Hexagonal Boron Nitride Nanosheets. *2D Mater.* **2020**, *7* (4), 045023.
- (35) Cholsuk, C.; Suwanna, S.; Vogl, T. Tailoring the Emission Wavelength of Color Centers in Hexagonal Boron Nitride for Quantum Applications. *Nanomaterials* **2022**, *12* (14), 1–13.
- (36) Ziegler, J.; Klaiss, R.; Blaikie, A.; Miller, D.; Horowitz, V. R.; Aleman, B. J. Deterministic quantum emitter formation in hexagonal boron nitride via controlled edge creation. *Nano Lett.* **2019**, *19*, 2121–2127.
- (37) Liu, Q.; Chen, C.; Du, M.; Wu, Y.; Ren, C.; Ding, K.; Song, M.; Huang, C. Porous Hexagonal Boron Nitride Sheets: Effect of Hydroxyl and Secondary Amino Groups on Photocatalytic Hydrogen Evolution. *ACS Appl. Nano Mater.* **2018**, *1* (9), 4566–4575.
- (38) Xiao, F.; Naficy, S.; Casillas, G.; Khan, M. H.; Katkus, T.; Jiang, L.; Liu, H.; Li, H.; Huang, Z. Edge-hydroxylated boron nitride nanosheets as an effective additive to improve the thermal response of hydrogels. *Adv. Mater.* **2015**, *27*, 7196–203.
- (39) Ren, J.; Stagi, L.; Innocenzi, P. Hydroxylated boron nitride materials: from structures to functional applications. *J. Mater. Sci.* **2021**, *56*, 4053–4079.
- (40) Wang, N.; Yang, G.; Wang, H.; Sun, R.; Wong, C. P. Visible Light-Responsive Photocatalytic Activity of Boron Nitride Incorporated Composites. *Front. Chem.* **2018**, *6*, 440.
- (41) Carboni, D.; Marongiu, D.; Russu, P.; Pinna, A.; Amenitsch, H.; Casula, M.; Marcelli, A.; Cibin, G.; Falcaro, P.; Malfatti, L.; Innocenzi, P. Enhanced Photocatalytic Activity in Low-Temperature Processed Titania Mesoporous Films. *J. Phys. Chem. C* **2014**, *118*, 12000–12009.
- (42) Ren, J.; Stagi, L.; Malfatti, L.; Garroni, S.; Enzo, S.; Innocenzi, P. Boron Nitride–Titania Mesoporous Film Heterostructures. *Langmuir* **2021**, *37*, 5348–5355.
- (43) Ren, J.; Innocenzi, P. 2D Boron Nitride Heterostructures: Recent Advances and Future Challenges. *Small Structures* **2021**, *2*, 2100068.
- (44) Angizi, S.; Hatamie, A.; Ghanbari, H.; Simchi, A. Mechanochemical green synthesis of exfoliated edge-functionalized boron nitride quantum dots: Application to vitamin c sensing through hybridization with gold electrodes. *ACS Appl. Mater. Interfaces* **2018**, *10*, 28819–28827.
- (45) Kainthola, A.; Bijalwan, K.; Negi, S.; Sharma, H.; Dwivedi, C. Hydrothermal synthesis of highly stable boron nitride nanoparticles. *Mater. Today. Proc.* **2020**, *28*, 138–140.
- (46) Fan, L.; Zhou, Y.; He, M.; Tong, Y.; Zhong, X.; Fang, J.; Bu, X. Facile microwave approach to controllable boron nitride quantum dots. *J. Mater. Sci.* **2017**, *52*, 13522–13532.
- (47) Lei, Z.; Xu, S.; Wan, J.; Wu, P. Facile preparation and multifunctional applications of boron nitride quantum dots. *Nanoscale* **2015**, *7*, 18902–18907.
- (48) Stagi, L.; Ren, J.; Innocenzi, P. From 2-D to 0-D Boron Nitride Materials, The Next Challenge. *Materials* **2019**, *12*, 3905.
- (49) Angizi, S.; Shayeganfar, F.; Azar, M. H.; Simchi, A. Surface/edge functionalized boron nitride quantum dots: Spectroscopic fingerprint

of bandgap modification by chemical functionalization. *Ceram. Int.* **2020**, *46*, 978–985.

(50) Ren, J.; Malfatti, L.; Enzo, S.; Carbonaro, C. M.; Calvillo, L.; Granozzi, G.; Innocenzi, P. Boron oxynitride two-colour fluorescent dots and their incorporation in a hybrid organic-inorganic film. *J. Colloid Interface Sci.* **2020**, *560*, 398–406.

(51) Stagi, L.; Malfatti, L.; Zollo, A.; Livraghi, S.; Carboni, D.; Chiriu, D.; Corpino, R.; Ricci, P. C.; Cappai, A.; Carbonaro, C. M.; Enzo, S.; Khaleel, A.; Adamson, A.; Gervais, C.; Falqui, A.; Innocenzi, P. Phosphorescence by trapping defects in boric acid induced by thermal processing. *Adv. Optical Mater.* **2023**, 2302682.